Solution Behavior of Normal and Reverse Triblock Copolymers (Pluronic L44 and 10R5) Individually and in Binary Mixture

ARTICLE *in* LANGMUIR · APRIL 2012

Impact Factor: 4.46 · DOI: 10.1021/la3000729 · Source: PubMed

3 AUTHORS, INCLUDING:

Bappaditya Naskar
Institut de Chimie Séparative de Marcoule
18 PUBLICATIONS **164** CITATIONS
SEE PROFILE

Satya P Moulik
Jadavpur University
297 PUBLICATIONS **7,343** CITATIONS
SEE PROFILE

Langmuir

Article

pubs.acs.org/Langmuir

Solution Behavior of Normal and Reverse Triblock Copolymers (Pluronic L44 and 10R5) Individually and in Binary Mixture

Bappaditya Naskar, Soumen Ghosh, and Satya P. Moulik*

Centre for Surface Science, Department of Chemistry, Jadavpur University, Kolkata 700032, India

ABSTRACT: Solution properties of pluronics L44 or L [$(PEO)_{10}(PPO)_{23}(PEO)_{10}$] and 10R5 or R [$(PPO)_8(PEO)_{22}(PPO)_8$] were studied individually as well in their binary mixtures in aqueous medium. The critical micelle concentration (CMC), critical micelle temperature, and cloud point (CP) were determined. Ideal and nonideal behaviors of their mixtures in the formation of CMC and CP were observed; the energetics of the studied processes were determined. Spectrophotometry, isothermal titration calorimetry and dynamic light scattering (DLS) methods were used for evaluations. Morphologies of the dispersed L, R, and their mixtures along with their polydispersities were determined from DLS measurements. Atomic force microscopy was also employed. The interfacial properties of L and R were investigated forming Langmuir monolayers in a surface balance. The surface pressures (π) generated by the compounds were moderate, the area per molecule was higher for R than L. R has shown antibacterial activity against both gram positive and gram negative bacteria whereas L was inactive in this respect.

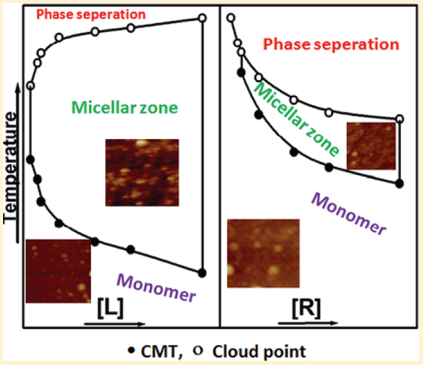

1. INTRODUCTION

Triblock copolymers of poly(ethylene oxide) (PEO) and poly(propylene oxide) (PPO) in the forms of PEO-PPO-PEO (normal pluronic) and PPO-PEO-PPO (reverse pluronic) have immense industrial applications in detergency, biomedical and pharmaceutical fields for their unique solution behavior, core−shell aggregate formation, phase behavior, dispersion stabilization, lubrication, low-toxicity, and minimal immune response.[1−8] Besides, they are also used in food protection, tissue engineering, coating and painting.[9−14]

Solution properties of pluronics are drastically changed with concentration and temperature by influencing their hydrophobic/hydrophilic character.[15−18] Due to differences in solubility of the constituent blocks, these copolymers show self-assembly characteristics in aqueous solution.[16−18] Their aggregation process is accentuated at higher temperature as both blocks lose solubility. Below the critical micelle temperature (CMT), both the blocks (PPO and PEO) are soluble in water in their monomeric forms. At the critical micelle concentration (CMC) as well as at CMT, their assemblies have the PPO block as the hydrophobic core and the hydrated PEO block as the corona.[17] As per reports, the nanoparticle properties are improved when they are prepared in solution in triblock copolymer aggregates; their biocompatibility and stability also improve.[19,20] On heating, the aqueous solution of pluronics beyond CMT clouds at a threshold temperature called the cloud point, CP[21,22] (depending on the concentration and environment), forming two coexisting isotropic phases. It has importance in understanding the instability of the pluronics in solution and the related thermodynamics. In many chemical processes clouding compounds are used alone or in mixture for effective solubilization, reaction, separation, and product formation.[23,24] Clouding of a species is generally attributed to the efficient dehydration of its hydrophilic portion at higher temperature.[21,25] Both increase and decrease in CP of pluronics with concentration are reported.[21,26−28]

Membrane sealing can be facilitated with the help of synthetic polymeric surfactant. A typical triblock copolymer (Poloxamer 188 or Pluronic F68) was reported to squeeze membrane and make it suitable for use.[29] Yasuda et al.[30] have demonstrated that in vivo administration of Pluronic F68 to dystrophic mice could lead to the improvement of the ventricular geometry and the blockade of acute cardiac failure. Thus, effective interaction of pluronics with biological membranes has been indicated.[31] Although the interfacial behavior of normal pluronics has been studied, that of reverse pluronics remains unexplored. We may herein mention that Mandal et al.[33,34] have studied the aggregation characteristics of both water-soluble and insoluble triblock copolymers in the presence of SDS micelles using a number of techniques which was a significant addition in the area of physicochemistry of pluronics, since studies on insoluble pluronics are much less frequent.

PPO/PEO category pluronics with a large variety of compositions and molar masses are commercially available. The information given in the introduction reveals that physicochemistry of normal pluronics (PEO/PPO/PEO) has been well studied[21−36] and is still being studied because of its multiple chemical, biochemical, and industrial uses. On the other hand, studies on reverse pluronics (PPO/PEO/PPO) have been less[37,38] than normal pluronics. The latter has good defoaming and wetting properties.[39] Phase behavior, aggrega-

Received: January 5, 2012
Revised: April 16, 2012
Published: April 16, 2012

   dx.doi.org/10.1021/la3000729 | Langmuir 2012, 28, 7134−7146

tion characteristics, performances in coating and painting as well as lubrication, templates for nanomaterial synthesis, etc. remain unexplored vis-a-vis normal pluronics. The interaction between normal and reverse pluronics can be also interesting and useful in terms of application. As per reports, pluronics and their mixtures may form gels,[40] and the field remains less explored. The gels formed by their combinations may find multiple uses in pharmaceutics, foods, physico-chemical processes, etc. The clouding, micellization, and morphology of their aggregates are expected to bring new information and directions for applications. Such studies are considered basics toward the understanding of more complicated multicomponent systems encountered in practice.

In this work, we have explored the solution behavior of the normal pluronic L44 (or L) and the reverse pluronic 10R5 (or R) and their mixtures. Both are closely similar in chemical composition with minor difference in their molar mass. The solution properties (CP, CMT, and CMC) of L and R and their mixtures have been studied in wide range of concentrations. The formation of their monolayer at the air/water interface has been also studied using a Langmuir balance. The morphological states of L and R in aqueous solution have been investigated by dynamic light scattering (DLS) and atomic force microscopy (AFM). The antibacterial activities of the pluronics have been tested toward Gram positive and negative bacteria.

2. MATERIALS AND METHODS

2.1. Materials. The triblock copolymers Pluronic L44 or L [$(PEO)_{10}(PPO)_{23}(PEO)_{10}$, molar mass 2200 g mol^{-1}] and 10R5 or R [$(PPO)_8(PEO)_{22}(PPO)_8$, 1950 g mol^{-1}] were donated by BASF (India) and were used as received. Pluronics normally contain low amounts of diblock copolymers as impurities in them. 1,6-Diphenyl-1,3,5-hexatriene (DPH) used was an AR grade product of Sigma (India). Doubly distilled water (κ = 2−4 μScm^{-1} at 30 °C) was employed for solution preparation.

The pluronic samples L and R used in this study were initially desiccated to remove the sorbed water in them. After desiccation to constant weight, they have shown the presence of 0.364 and 0.167 wt % water in L and R, respectively. The samples were kept in desiccating condition unless required for use.

2.2. Methods. *2.2.1. Absorbance.* Absorbance measurements were taken in a UV 1601 Shimadzu (Japan) spectrophotometer using 10 mm path length matched quartz cuvettes. In the determination of CMC, DPH was used as the probe at concentration 0.1 μM. The spectra were recorded at different [pluronic] by adding a concentrated aqueous pluronic solution containing 0.1 μM DPH in multiple steps and measuring the absorbance in each step after thorough mixing and equilibration.

For the determination of CMT, a desired concentration of pluronic solution was placed in the cuvette containing [DPH] (used as a probe) = 0.1 μM, and the temperature was increased from 15 to 60 °C, in steps taking measurements allowing time for equlibration. The absorbance measurements were taken at 356 nm for the estimation of both CMC and CMT.

2.2.2. Microcalorimetry. An OMEGA isothermal titration calorimeter (ITC) of Microcal, Northampton (U.S.A.) was used for thermometric measurements. During measurements, temperature was kept constant by circulating water from a Neslab RTE100 (U.S.A.) water bath at 5 °C below the temperature in the calorimetric cell as per procedural requirement. The temperature in the calorimetric cells was accurate within ±0.01 °C. The heat released or absorbed at each step of dilution of pluronic solution in water and the enthalpy change per mole of injectant was calculated with the help of the ITC software. The reproducibility was checked from repeat experimentations. The required ΔH^0_m was calculated following the procedure described elsewhere.[41]

2.2.3. Cloud Point (CP) Determination. The experimental procedure for cloud point (CP) determination previously reported[21,22] was followed. The measuring solution was taken in a securely stoppered thin glass test tube and placed in a heating mantle having arrangement for constant stirring and controlled increment of heat. The point of starting of clouding (turbidity) was visually observed and recorded. The heating was then stopped, and the system under stirring condition was allowed to cool slowly. The temperature for the disappearance of turbidity was also noted. The mean value of the two temperatures was considered as the CP of the system. The measured CP was accurate within ±0.5 °C.

2.2.4. Surface Pressure−Area (π−A) Isotherm. The π−A isotherms of the pluronics at the air/water interface were obtained in a Teflon-bar-barrier type Langmuir−Blodgett trough (model −2004C, Apex Ins. Co., India).[42] Doubly distilled water (resistivity of 18.2 MΩ cm) was used as the subphase. The temperature was controlled at 25 ± 1 °C. Initially, the pluronics were dissolved in $CHCl_3$. A total of 75 μL of the 0.1 mg mL^{-1} solution of the pluronic was then spread with a microsyringe (Hamilton, U.S.A.) at the air/water interface on the aqueous subphase (area, 450 cm^2, volume, 275 mL). We allowed 30 min for the evaporation of solvent and equilibration of monolayer at the air/water interface. The monolayer was then compressed with a speed of 5 mm min^{-1}. The changes in the surface pressure (π) were measured by using a film electro balance (Sartorius) of resolution 0.01 mN m^{-1} connected with a computer. Measurements were duplicated for checking reproducibility of the data.

2.2.5. Dynamic Light Scattering (DLS). DLS measurements were taken at 173° angle in a Malvern Zetasizers Nanozs apparatus with a He−Ne laser (λ = 632 nm) at 30 °C. The sample cells were placed in a temperature- controlled, refractive index matched bath filled with cis−trans decahydronaphthalene (decalin). All solutions were filtered 3−4 times through membrane filters (porosity 0.25 μm) to remove dust particles. The mean values of duplicate experiments were reported.

2.2.6. Atomic Force Microscopy (AFM). The topological images of the pluronic samples on glass slides were taken with a NT-MDT AFM in noncontact mode with a constant force of 20 mN. The hydrophilic glass surfaces were cleaned in dilute piranha solution consisting of water, sulphuric acid (98%), and hydrogen peroxide (27.5% solution in water) in a 5:4:1 volume ratio at 80 °C for 30 min, which provided effective cleaning yet preserved the low roughness of the native oxide layer. A drop of the pluronic solution was placed onto the glass surface, and it was dried by slow heating followed by cooling and taking measurements.

2.2.7. Antibacterial Activity. The antibacterial activities of the pluronic against *Escherichia coli* and *Staphylococcus aureus* were evaluated by using colony counting method as described elsewhere.[43] A representative colony was taken out for preparation of bacterial cell culture with the help of a wire loop and placed in nutrient broth (peptone 10 g, beef extract 3 g, NaCl 3 g in distilled water 1000 mL; pH 7.0) for overnight incubation at 37 °C. After that the nutrient agar containing plate was prepared which contained 10 mM samples of L and R. The overnight incubated bacterial culture broth appropriately diluted with sterile distilled water containing ca. 102 cell/mL was used for antibacterial activity behavior by spread plate technique. The colonies were counted after overnight incubation at 37 °C. All of the data were expressed as three replications with colony forming unit (CFU), and one way ANOVA program was used for the statistical analysis. The values were considered to be significantly different when probability, $p > 0.01$.

3. RESULTS AND DISCUSSION

3.1. Micellization Behavior. The self-aggregation (i.e., micellization) of block copolymer chains in solutions can generally be studied either initiated by increasing concentration (where micelles form at a critical micelle concentration, CMC at a fixed temperature) or by changing the temperature (micelles also form at a critical micelle temperature, CMT at a fixed concentration). Both CMC and CMT are the

dx.doi.org/10.1021/la3000729 | Langmuir 2012, 28, 7134−7146

fundamental parameters which characterize the self-assembly of pluronics in solution.

3.1.1. CMC of L. Pluronics aggregate in solution after a certain concentration forming multimeric assembles (micelles) at and above CMC.[16−18] For the determination of CMC, spectral measurements of a hydrophobic dye like DPH in pluronic solution were taken. This probe can also be used for the determination of CMT and other physical properties like membrane fluidity, dynamic phenomena of vesicles, etc.[17] DPH absorbs weakly in water and strongly in hydrophobic enviornment, showing a characteristic peak at 356 nm.[17] A typical plot of spectra of DPH (at 55 °C) with increasing concentration of L is presented in the inset of Figure 1A.

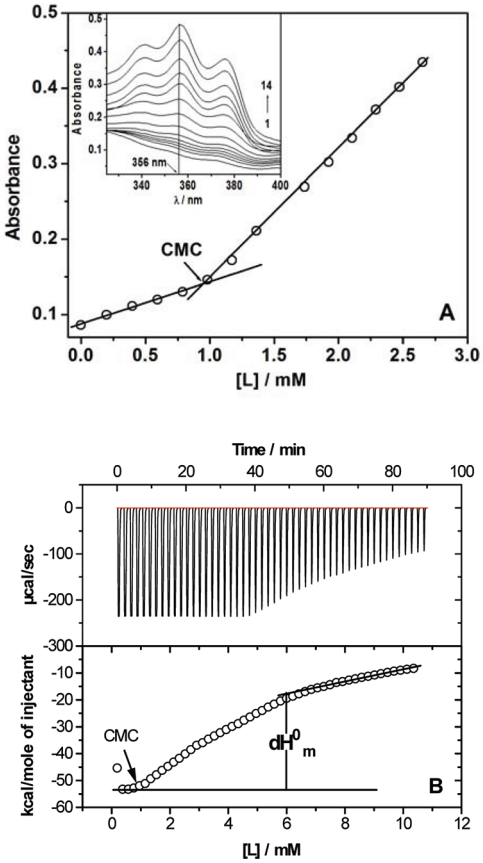

Figure 1. (A) Spectrophotometric determination CMC of L at 55 °C. Inset: Basic spectra of DPH at 55 °C with increasing concentration of L, 1 → 14; 0, 0.20, 0.40, 0.59, 0.79, 0.98, 1.17, 1.36, 1.74, 1.92, 2.11, 2.29, 2.47, and 2.65 mM. (B) Enthalpogram of dilution of L in water at 55 °C. Top: Calorimetric traces (heat flow against time). Bottom: Process enthalpy versus [L] profile. The CMC is marked on the profile; ΔH^0_m is represented by the length of the line.

Micellization of normal pluronics determined by spectrophotometry and light scattering methods is well documented in the literature.[16,17,44] Herein ITC method was also used to study pluronic L micellization along with spectrophotometry; ITC was very limitedly used in pluronic study.[45,46] Representative absorption and ITC graphs of L at 55 °C are presented in Figure 1. The CMC points are indicated by arrowheads in the figure along with the rationale of estimation of the standard enthalpy of micellization (ΔH^0_m). The same protocol was also used by Taboada et al.[47a] on poly(oxypropylene)−poly(oxyethylene) diblock copolymer and Winnick et al.[47b] on polymeric surfactant. Like us Taboada et al.[47a] also found a less sharp long intermediate region between the start and completion of micellization of pluronic (cf, Figure 1). We considered this phenomenon as the result of concentration dependent change in aggregation number affecting the monomer ⇌ micelle equilibrium in the region, as the temperature dependent broad peak of the DSC curve of pluronic L64 was described on the basis of changed monomer ⇌ micelle.[26] Both temperature and concentration dependent aggregation number are reported above CMC for normal pluronics L64[48a] and P123,[48b] respectively. For L64[48a] at 2.5 wt %, the aggregation number increased from 37 to 45 in the temperature range of 37.5 to 55 °C: for P123[48b] the aggregation numbers were 88 and 99 at 50 °C for 4 and 6 wt % of the compound, respectively. The CMC values of L herein obtained by the two methods are given in Table 1, and the values showed good agreement. The CMC of L was reported to be 3.6 mM in assay buffer (pH 7.4) at 37 °C.[49]

Table 1. Temperature Dependent CMC and Energetic Parameters of L in Aqueous Medium

	CMC/mM					
T/°C	Abs	Mcal	Ave	$-\Delta G^0_m$/ kJ mol^{-1}	ΔH^0_m/ kJ mol^{-1}	ΔS^0_m/J mol^{-1} K^{-1}
48	4.10	3.91	4.00	25.5	57.6	259
50	2.28	2.35	2.32	27.1	78.8	328
52	1.69	1.61	1.65	28.2	113	436
55	0.97	0.95	0.96	29.9	164	592

In the evaluation of energetics of micellization, the standard enthalpy of micellization (ΔH^0_m) values were directly obtained from ITC experiments. The standard free energy change (ΔG^0_m) and standard entropy change (ΔS^0_m) of micellization were calculated from the following relations 1 and 2 given below.

$$\Delta G^0_m = RT \ln X_{\text{pluronic}} \quad (1)$$

where X_{pluronic} is the mole fraction concentration of pluronic.

$$\Delta S^0_m = (\Delta H^0_m - \Delta G^0_m)/T \quad (2)$$

The standard enthalpy change of micellization can also be obtained by van't Hoff rationale.

$$\frac{d(\Delta G^0_m/T)}{d(1/T)} = \Delta H^0_m \quad (3)$$

The CMC of L decreased with temperature (Table 1) making ΔG^0_m more negative. Lowering of hydration of the nonionic L caused easier self-aggregation and decrease of CMC with increasing temperature (cf Table 1).[17] Endothermic ΔH^0_m (found from ITC) increased with increasing temperature as generally found for pluronics.[45] Processing the ΔG^0_m data of Table 1 in terms of the van't Hoff rationale (eq 3), ΔH^0_m= 175 kJ mol^{-1} was obtained, which was larger than all the ITC determined values. The estimated ΔS^0_m values were all large and positive. Similar discrepancy was also reported by Li et al.[50] for F127. Surfactant micellization has been reported to produce non equivalent enthalpy values determined by the van't Hoff and by calorimetry (ITC). In the van't Hoff method only the equilibrium process, nL ⇌ L$_n$ (where n represents the number of monomer of L) is considered in the treatment to estimate ΔH^0_m. In ITC, all kinds of heat (like solvation−desolvation,

dx.doi.org/10.1021/la3000729 | *Langmuir* 2012, 28, 7134−7146

solvent structure breaking−making, dissociation−association, morphological changes of the ensembles, etc.) are measured, and the result is registered to get ΔH^0_m; obviously the thermodynamic parameters depend on temperature. The former is therefore a differential process, whereas the latter (ITC) is an integral process. A detailed discussion can be found in the work of Moulik and Mitra.[51] Like conventional surfactant, the magnitude of micellization depends on pluronic structure.[45,51] The micellization process was spontaneous with a large entropy change. According to Bouchemal et al.,[45] the large entropy gain was due to release of water molecules from the hydration shells around the hydrophobic parts of the monomer. ΔH^0_m and ΔS^0_m compensated each other; the compensation temperature for L micellization was 48 °C, whereas the average experimental temperature was 49.3 °C (correlation coefficient = 0.999; plot not shown to save space). We were unable to determine the CMC of R by ITC for its high value and solubility reason restricting preparation of the concentrated solution. Getting CMT for R at different concentrations (which is equivalent to CMC at the CMT condition) is a convenient way to study self-aggregation of pluronics. This is presented in the next section.

3.1.2. CMT of L and R. Spectrophotometry and DLS measurements were employed to determine CMT. A typical plot of spectra of DPH (in 20 mM of R) with increasing temperature is presented in the inset of Figure 2; the absorbance versus temperature plots (for L, R, and their 1:1 mixture) are illustrated in the main plot from which CMTs were determined considering the first inflection. The results are presented in Table 2. The CMT of normal pluronics in water determined by light scattering, differential scanning calorimetry, spectrophotometry, NMR, etc. are reported.[17,37,52] However, a question arises about the micellization of reverse pluronics. Alexandridis et al.[18] reported the nonmicellization behavior of 25R4 by surface tension measurements, although normal pluronics show clear micellization by the tensiometry method. D'Errico et al.[39] did not find any transition from NMR self-diffusion data of 25R4 which could be related with CMC. In concentrated solution, the diffusion coefficient obtained from NMR became extremely low, indicating stronger intermolecular interaction between the copolymer chains indicating formation of some structure. This and the presence of a cloudy region in the solution suggested the formation of micellar aggregates of the 25R4−water system. The transition between monomer and interconnected micelles was not sharp, restricting the detection of CMC of the reversed pluronic. Zhou et al.[37] reported micellization of R pluronic by light scattering method and also described its concentration dependent CMT like normal pluronics in aqueous solution. Herein, we also observed temperature dependent transition for the CMT of R like. The CMT values of the studied L were lower than those of the reverse pluronic R; CMTs of their mixtures were inbetween. They followed the order L < 4L:1R < 1L:1R < 1L:4R < R. Thus, L was a better micelle forming copolymer than R.

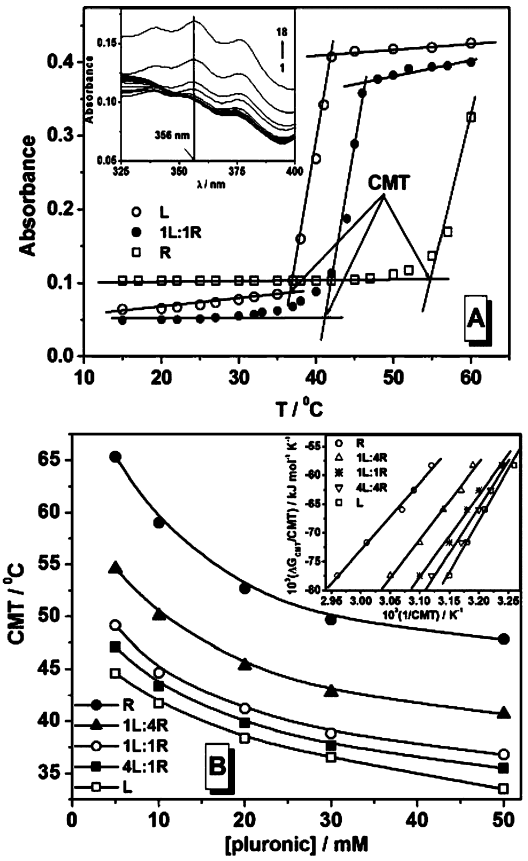

Figure 2. (A) DPH absorbance vs temperature to determine CMT of L, R, and 1L:1R of 20 mM. Inset: Spectra of DPH of 20 mM R with increasing temperature. Curves, 1 → 18; 15, 20, 25, 27, 30, 32, 35, 38, 40, 42, 45, 47, 50, 52, 55, and 57 °C. (B) Concentration dependent CMT of L, R, and their mixtures. Inset: van't Hoff plot of ΔG_{CMT}/CMT vs 1/CMT for the determination of ΔH_{CMT}.

We considered the solution concentration associated with each CMT as the CMC at that temperature and used relations equivalent to eqs 1−3 considering an association model in terms of equilibrium between molecularly dispersed copolymer (monomer) and multimolecular aggregates (micelles), to get ΔG_{CMT}, ΔH_{CMT}, and ΔS_{CMT}. The plot between (ΔG_{CMT}/CMT) against (1/CMT) was linear (inset, Figure 2B), whose slope yielded ΔH_{CMT} given in the footnote of Table 2 with ΔG_{CMT} and ΔS_{CMT}. The self-aggregation of the pluronics was endothermic and associated with large entropy change. By the above procedure, Alexandridis et al.[17] also reported the ΔH_{CMT} for various normal pluronics (PPO/PEO ≈ 1.15) in the 200−300 kJ mol^{-1} range. In the present study, ΔH_{CMT} of L (PPO/PEO ≈ 1.15) and R (PPO/PEO ≈ 0.73) were 174 and 115 kJ mol^{-1}, respectively. Strikingly, our enthalpy value of R was exactly matched with 17R5 (115 kJ mol^{-1}) reported by Zhou et al.[37] The endothermic ΔH_{CMT} indicated that the transfer of monomer from water to micellar aggregate occurred by disruption of the adjacent water structure as well as the micellar structure producing positive entropy change.[18] Usually, the entropy contribution dominates for normal/conventional surfactant micellization,[51] but for the block copolymers, the process was fairly controlled by both enthalpy and entropy. In comparison, the energetic parameters of R were higher than those of L because of its higher PEO content.

3.1.3. Mixed Micelle Formation. Solution properties of mixed surfactant systems are interesting and useful both from physicochemical and application view points. Ionic surfactants, such as sodium dodecyl sulfate (SDS),[53a] cetyltrimethylammonium bromide (CTAB),[53b] and cetyltrimethylammonium chloride (CTAC),[53c] are often added into the aqueous solution of copolymer to observe their effect on the self-aggregation behavior of the pluronics. It is found that SDS usually prevents micellization of copolymer, and binds with it to form complex. On the other hand, nonionic surfactants, including hexa-

dx.doi.org/10.1021/la3000729 | Langmuir 2012, 28, 7134−7146

Table 2. Concentration Dependent CMT and Energetic Parameters of L, R, and Their Mixtures

[pluronic]/mM	CMT/°C					ΔG_{CMT}/kJ mol^{-1} (ΔS_{CMT}/kJ mol^{-1} K^{-1})				
	L	4L:1R	1L:1R	1L:4R	R	L	4L:1R	1L:1R	1L:4R	R
5	44.6	47.3	49.5	54.6	65.3	−24.6 (0.625)	−24.8 (0.589)	−25.0 (0.531)	−25.4 (0.496)	−26.2 (0.418)
10	41.2	42.4	44.4	50.1	58.7	−22.5 (0.625)	−22.6 (0.592)	−22.8 (0.532)	−23.2 (0.496)	−23.8 (0.419)
20	38.3 (38)[b]	39.7	41.2 (41)[b]	45.35	52.7 (52)[b]	−20.5 (0.623)	−20.6 (0.590)	−20.7 (0.531)	−21.0 (0.497)	−21.5 (0.420)
30	37.1	38.0	39.2	42.8	50.3	−19.4 (0.623)	−19.5 (0.590)	−19.5 (0.531)	−19.8 (0.497)	−20.2 (0.419)
50	33.5 (32)[b]	35.5	36.1 (35)[b]	40.7	47.8 (48)[b]	−17.8 (0.625)	−18.0 (0.590)	−18.0 (0.531)	−18.3 (0.496)	−18.7 (0.418)

[a]The ΔH_{CMT} were 174, 164, 146, 137, and 115 kJ mol^{-1} for L, 4L:1R, 1L:1R, 1L:4R, and R, respectively. The ΔH_{CMT} for L by van't Hoff was 155 kJ mol^{-1} determined by combining CMT and CMC (see text). [b]DLS results.

ethylene glycol mono-*n*-dodecyl ether ($C_{12}EO_6$),[53d] Triton X-100,[53e] etc., promote micellization of the copolymer. The literature is rich with mixed systems of conventional surfactants and their combinations with pluronics, but to the best of our knowledge, studies on normal and reverse mixed pluronics still remain unexplored. L and R mixed in different proportions at 50 °C produced mixed micelles; their CMCs are given in Table 3. The nature of the interaction between L and R in the mixed micelles can be understood in terms of Clint equation for ideal mixing. Thus

Table 3. Mixed Micellization Behavior of L and R at 50 °C Determined by Spectrophotometry

	CMC/mM	
X_R	expt	Clint
0	2.28	2.28
0.2	3.10	2.80
0.5	4.57	4.23
0.8	10.0	8.74
1.0	30.0	30.0

$$\frac{1}{CMC_{mix}} = \frac{X_L}{CMC_L} + \frac{1 - X_L}{CMC_R} \quad (4)$$

where CMC_L, CMC_R, and CMC_{mix} are the CMCs of L, R, and their mixtures, respectively, and X_L is the mole fraction of L in solution.

The CMC_{mix} values found from eq 4 are given in Table 3 along with the experimental values and compairing them in Figure 3. A nonideal mixture (components interacting) would show deviation from the equation, and the CMC_{mix} could be both lower and higher than Clint's prediction for synergism and antagonism, respectively. The experimental results fitted well with Clint's rationale with a minimal deviation, suggesting an ideal behavior of the mixed pluronics (L and R) in the mixed micelle. The ideal mixed micelle formation was reported[54] for mixed conventional surfactants like tetradecyltrimethylammonium bromide−cetyltrimethylammonium bromide and sodium dodecylsulfate−sodium dodecylbenzenesulfonate; mixed pluronic-normal surfactant exhibited nonideality.[55,56]

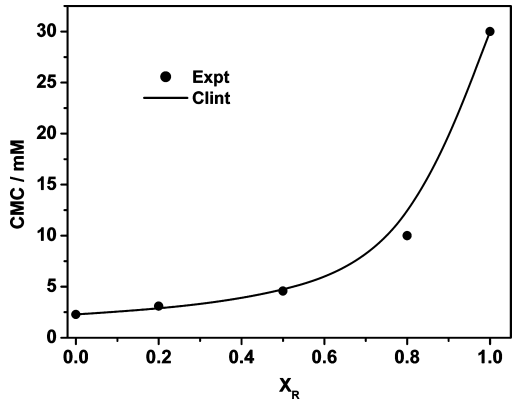

Figure 3. Dependence of CMC on stoichiometric X_R for the L−R system at 50 °C. The curve by Clint equation; the points are experimental.

3.2. Cloud point (CP). CP measurement of pluronics is an effective way of understanding their phase separation property. The clouding phenomenon of pluronic is interpreted by way of dehydration of the PEO moiety (loosening of hydrogen bonding between ethereal oxygen of PEO and water), and polar-nonpolar conformation change of PEO by the effect of temperature.[57] The concentration dependent CPs of aqueous solutions of L and R and their mixtures are presented in Figure 4A. The CP of L sharply increases from 62 °C (at 2 mM) up to 70 °C at 10 mM, and the increase thereafter is mild. At 50 mM, the CP of L was 73 °C. The CP of R decreases exponentially from 74 °C (at 2 mM) to 58 °C at 50 mM. The following relation was found to describe the concentration dependent CP of L (correlation coefficient = 0.982).

$$CP_L = e^{a+b/c+x} \quad (5)$$

where a, b, and c are constants and x is the concentration of L (a = 4.29, b = −0.56, and c = 1.52).

The relation for R (correlation coefficient = 0.999) was

$$CP_R = a' + b'e^{-x/t_1} + c'e^{-x/t_2} \quad (6)$$

where a', b', c', t_1, and t_2 are constants and x is the concentration of R (a' = 51.61, b' = 9.71, c' = 14.75, t_1 = 2.08, and t_2 = 13.23).

Such equations were not used in the past to describe the CP dependence on [pluronic]. It can be added that we have tested eqs 5 and 6 and found that they fairly satisfy the concentration dependent CP of L64[26] ($(PEO)_{13}(PPO)_{30}(PEO)_{13}$) and 31R1[58] ($(PPO)_{27}(PEO)_4(PPO)_{27}$), respectively, with different magnitudes of the constants. The equations, therefore, have a generality; more studies are required in this context.

CP of normal pluronics decreases with increasing concentration; increase in CP with concentration has been also reported for L64[26] and P65.[53] Zhou et al.[37] reported decreased CP with increased [17R4] (reverse pluronic) up to a certain concentration, and then it slightly increased. We have observed increased CP with increased [L] and decreased CP with increased [R]. For an equimolar mixture of L and R, CP initially decreased followed by a sharp increase up to 10 mM. The minimum depended on the mole ratio; increasing proportion of R shifted the minimum to higher concentration

dx.doi.org/10.1021/la3000729 | Langmuir 2012, 28, 7134−7146

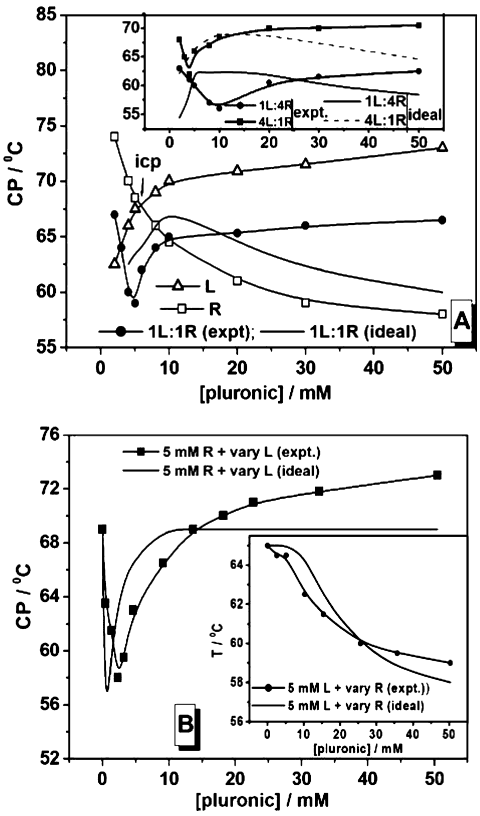

Figure 4. (A) Concentration dependent clouding behavior of L, R, and their mixtures. Inset: Same plot for 1L:4R and 4L:1R. (B) Clouding behavior of 5 mM R with varying L. Inset: Same plot for 5 mM L with varying R.

since the trends of their individual CPs with respect to concentration were opposite. The CP values of L affected by [R] and vice versa are presented in Figure 4B. The result was strikingly different from that of the influence of L on R. The temperature induced dehydration of the efficiently solvated ethylene oxide moiety in the peripherial region of L, and the weakly solvated outer region of R assemblies are the suggested models as presented in Figure 5, panels A and B, to explain the CP dependence on [pluronic] discussed below.

In L, the PPO/PEO ratio is 1.2 which is 0.72 in R; R is therefore, more soluble in water than L. The clouding is thus easier in L than in R so that their CP values are 62.5 and 74 °C, respectively at 2.0 mM concentration (see Figure 4A and Table 4). The morphologies of the micellar assemblies of L and R are shown in Figure 5, panels A and B; the former (L) has a hydrophilic mantle (which remains hydrated), whereas the latter (R) has hydrated hydrophilic outer segments of PEO units attached with hydrophobic PPO interior in the form of star like species. At a low concentration, increasing temperature desolvates L micelles with a point of clouding that is CP where solvent depleted individual units assemble to form a separate phase. At a moderate concentration of L, several micelle units remain assembled in solution trapping water in the three-dimensional structure whose removal requires extra energy causing rise in CP. In the higher concentration range, clustered assemblies of still higher sizes form in solution trapping greater amounts of water thereby requiring higher amounts of heat to manifest further rise in CP that tends to level off at [L] ≈ 50 mM. Above 50 mM the interplay of configurational, thermal, and entropic effects minimize formation of higher assemblies in solution. On the other hand, the species generated from R are more soluble and less assembled (lower aggregates supported by DLS results discussed latter). At low concentrations equivalent to that of L (2.0 mM), assembly formation of smaller and more soluble micelles by dehydration requires a higher temperature to augment clouding, and hence CP is larger than that of L. At moderate [R], population of the micellar units increases with augmentation of favorable clustering of the desolvated units causing a decline in CP. Formation of assemblies of R to trap water is not possible for want of easy interpenetration of the PPO linked PEO segments to form structures. The penetration of the PEO segments in the nonpolar cavity is also not possible for steric and polarity restrictions. The desolvated species thus produce adhered clusters which favorably form with increasing [R] making CP to continuously decline. This is supported by the entropy of clouding (discussed below) which is negative for L and positive for R; the dehydrated species interpenetrates to become ordered in L which is loose in R due to lack of interpenetration. The curves of L and R crossed at CP ≈ 62 °C at [L] = [R] = 5.8 mM which is the iso-cloud point marked as "icp" on the plot (Figure 4A).

The CP vs [pluronic] course of mixed L and R was much different from their individuals leading to the anticipation of interaction between L and R for the consequence. If we consider that L and R kept their individual identities in solution in respect of clouding (ideal behavior), then below icp the system should respond to the lower CP produced by L. In the post icp range, the CP of R should guide the phenomenon. With this rationale, based on the composition of the mixture, the symbol-less CP curve for the ideal (noninteracting) system

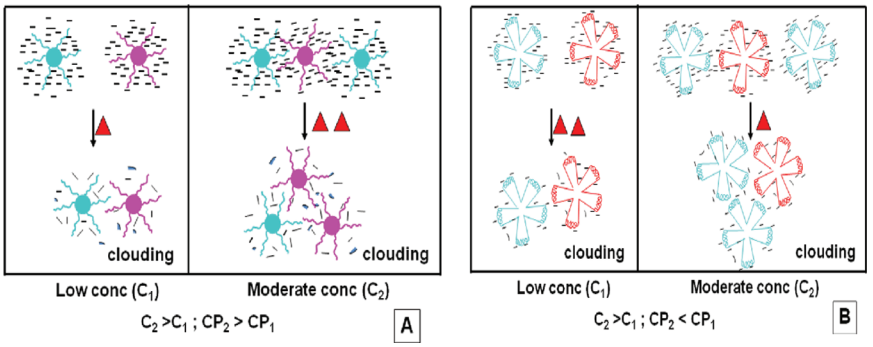

Figure 5. (A) Temperature effect on the clouding behavior of L. Desolvated species clustered by interperipheral penetration. (B) Temperature effect on the clouding behavior of R. Desolvated species clustered by group association.

dx.doi.org/10.1021/la3000729 | Langmuir 2012, 28, 7134−7146

Table 4. Energetics of Clouding of Pluronics L and R in Aqueous Media

	CP/°C		ΔG_c/kJ mol^{-1}		ΔH_c/kJ mol^{-1}		ΔS_c/kJ mol^{-1} K^{-1}	
[pluronic]/mM	L	R	L	R	L	R	L	R
2.0	62.5	74.0	−28.5	−29.5	−55.0	127	−0.08	0.45
4.0	66.0	70.0	−26.9	−27.2	−220	155	−0.57	0.53
5.0	67.5	68.5	−26.4	−26.5	−290	165	−0.77	0.56
8.0	69.0	66.0	−25.2	−24.9	−359	183	−0.98	0.61
10.0	70.0	64.5	−24.6	−24.2	−405	193	−1.11	0.65
20.0	70.9	61.0	−22.7	−22.0	−446	218	−1.23	0.72
30.0	71.5	59.0	−21.6	−20.8	−473	233	−1.31	0.77
50.0	73.0	58.0	−20.2	−19.3	−541	241	−1.51	0.79

has been constructed and presented in the diagram. The course evidenced a convex pattern with a maximum at [pluronic] = 10 mM; it did not merge with the CP curve of R but ran parallel with a constant difference of ∼2.5 °C. Such ideal mixing curves are also presented in the inset of Figure 4, panels A and B. The behaviors were similar. The appreciable difference between the constructed and the experimental patterns suggested non-ideality of the mixed systems in solution with respect to CP.

With consideration of clouding as the point of phase separation (or the solubility limit),[21] the free energy change of the process clouding (ΔG_c) was calculated using eq 7 (analogous to eq 1),[21] where X_C is the [pluronic] in mole fraction at the point of clouding. The calculated ΔG_c values are presented in Table 4. The enthalpy (ΔH_c), entropy (ΔS_c), and heat capacity ($\Delta C_{p,c}$) changes for the clouding process were evaluated from eqs 8−10, respectively.

$$\Delta G_c = RT \ln X_c \tag{7}$$

The plots between $(\Delta G_c/T)$ and $(1/T)$ were nonlinear (Figure 6). Hence, polynomial equation of the following form was used to calculate ΔH_c.

$$\frac{\Delta G_c}{T} = A + \frac{B}{T} + \frac{C}{T^2} \tag{8}$$

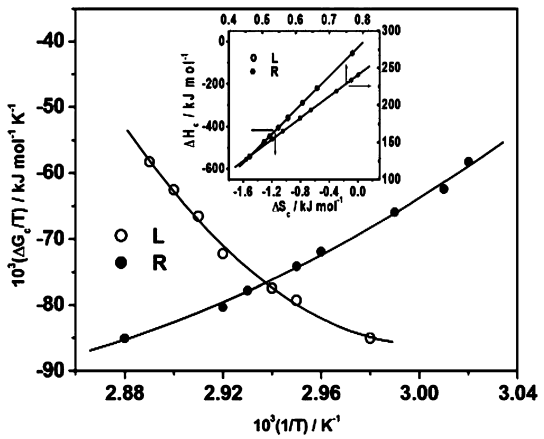

Figure 6. ΔG_c/CP vs 1/CP plot for the determination of ΔH_c. Inset: Compensation plot between ΔH_c and ΔS_c.

Thus

$$\Delta H_c = \frac{d(\Delta G_c/T)}{d(1/T)} = B + \frac{2C}{T} \tag{9}$$

with A, B, and C denoting the coefficients of the polynomial relation. The correlation coefficients of the fitting curves (Figure 6) were 0.984 and 0.996 for L and R, respectively.

Also

$$\Delta C_{p,c} = \frac{d\Delta H_c}{dT} \tag{10}$$

The above concept and equations were considered for understanding the energatics of the clouding of nonionic surfactants, water-soluble polymers, geminis, etc. individually as well as in presence of additives.[21]

Changes in the free energy of clouding for both of the pluronics were negative but enthalpy and entropy values were either negative or positive depending on the nature of the pluronic (Table 4). Positive enthalpy change was also reported from DSC experiments on reverse pluronic 31R1.[58] According to the above rationale, Prasad et al. reported[21a] an athermal clouding process of normal pluronic 85. In presence of hydrotopes, the ΔH_c became appreciably endothermic (∼100−600 kJ mol^{-1}) for pluronic 85. Methylcellulose, polyvinylmethyl ether, and Brij 56 showed ΔH_c values −251, −151, and −565 kJ mol^{-1}, respectively. The athermal TX-100 ended up in high endothermic ΔH_c (∼50−1000 kJ mol^{-1}) in the presence of a different proportion of saponin (acaciaside).[21c] The clouding of salt induced PVP (polyvinyl pyrolidone) was reported to be in the range of ∼140−350 kJ mol^{-1}.[22] The magnitudes of exothermic and endothermic ΔH_c for L and R, respectively, evidenced comparative enthalpic behavior. However, using the above energetic model Kabir-ud-din et al.[21b] determined the ΔH_c of hydroxypropylmethyl cellulose in presence of cationic surfactant (TTAB, DTAB, CTAB, and CPC), anionic surfactant (SDS), and gemini surfactants. The results were endothermic and much lower (∼4−20 kJ mol^{-1}). The heat capacities of L and R (obtained from the slopes of the ΔH_c vs T plots) were −46.3 and −7.10 kJ K^{-1} mol^{-1}, respectively. A negative heat capacity change (−21.4 kJ K^{-1} mol^{-1}) was also reported for 31R1.[58] This negative heat capacity change indicated the loss of structured water from the solvation sphere.[59] For both L and R, ΔH_c values were moderately lower than those of $T\Delta S_c$; therefore, both parameters effectively contributed to the clouding process. The ΔH_c and ΔS_c nicely compensated each other (Figure 6, inset) for both L and R; their compensation temperatures were 67.0 and 64.6 °C, respectively (the respective average experimental temperatures were 68.8 and 65.1 °C). We considered the hydration removed entities (pluronic aggregates) forming loose clusters for R with positive ΔS_c. Penetration of polar groups among the dehydrated entities made ΔS_c of L negative.

dx.doi.org/10.1021/la3000729 | Langmuir 2012, 28, 7134−7146

3.3. Monolayer Study. Pluronics are surface active.[18] We also studied the Langmuir monolayer of L and R at the air/water interface in a Langmuir balance. The $\pi-A$ isotherms are shown in Figure 7. Both L and R are water-soluble, and L has a

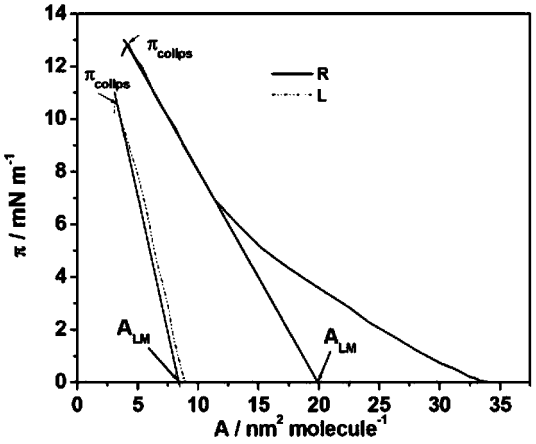

Figure 7. $\pi-A$ isotherm for L and R monolayers at 25 °C. π_{collps} = Collapse pressure of the film. A_{LM} = Limiting surface area per molecule of the pluronic.

greater polarity than R. We considered that within 30 min after their application on the undisturbed sub phase they very minorly dissolved and their π-A isotherms stood for their total mass added at the interface. The surface pressure steeply rose from the beginning for L, and it was initially less steep but fairly so at the later stage for R, and they collapsed at 10.43 and 12.81 mN m^{-1}, respectively. The calculated limiting surface areas (from the drawn tangents up to the x axis) occupied per molecule was 19.92 and 8.32 nm^2 for R and L, respectively. Alexandridis et al.[18] tensiometrically studied the interfacial behavior of normal pluronics (with PPO/PEO ratio, 0.77−1.79) in terms of Gibbs monolayer and reported the molecular area (A_{Gibbs}) in the range of 0.50−1.52 nm^2 $molecule^{-1}$ at 25 °C. The values were considerably lower than (7−13 nm^2 $molecule^{-1}$) that were obtained by Chang et al.[60] from Langmuir monolayer (LM) measurement on pluronics (with PPO/PEO ratios 0.2−1.5). Our A_{LM} values of L and R (with PPO/PEO ratios 1.4 and 1.2, respectively) matched with the results of Chang et al.[60] The larger A_{LM} values of L and R meant flat orientation of L and R at the interface; the area described by R was greater than L at the interface. Much lower values of A_{Gibbs} reported by Alexandridis et al.[18] cast doubt on the validity of Gibbs equation on pluronics solution (their γ vs log[pluronic] profiles were different from conventional surfactant) with two breaks. The post first break courses were much less steep and wavy. For polydisperse commercial pluronics (usually with diblock impurities) showing uncommon tensiometric behavior, estimation of A_{Gibbs} from the initial linear course well below CMC is doubtful. It ought to be greater than actual for the monolayer formation was not with complete surface coverage like that occurs at CMC. But the reported results were unexpectedly much lower.

Considering the −C−C− and −C−O− bond distances, the calculated length of a fully stretched PPO unit is 0.3 nm. If the $(PPO)_{23}$ and $2(PPO)_8$ hydrophobic polymeric parts of L and R are taken to remain at the interface, then they should describe circular areas of 38.5 and 18.1 nm^2 $molecule^{-1}$, respectively. The experimental results for L (8.32 nm^2 $molecule^{-1}$) were much smaller than the calculated value, whereas for R, the experimented value (19.9 nm^2 $molecule^{-1}$) was close to the calculated value (18.1 nm^2 $molecule^{-1}$). This suggested that the long $(PPO)_{23}$ segment in L folded to assume a small stable configuration at the interface which the two relatively small (PPO) segments could not perform being separated by the water surrounding $(PEO)_{22}$ segment for steric reasons. The above rationale and results were tentative but the derived trends and magnitudes were instructive.

Gibbs free energy change due to compression of the pluronics' monolayer (ΔG_{cm}) was obtained using eq 11.

$$\Delta G_{cm} = \int_{A_1}^{A_2} \pi \, dA \tag{11}$$

where A_1 and A_2 are the start and end of compression (before collapse).

ΔG_{cm} is the work required to compress a monolayer (which is a measure of the intermolecular forces in the film). ΔG_{cm} values found for L and R were 211 and 1104 kJ mol^{-1}. This implied that higher energy was required for compressing the monolayer of R than that of L. The ΔG_{cm} is dependent on the interaction between the type of molecules present in the monolayer and the subphase. As an example we mention that Talapatra et al.[61] reported the ΔG_{cm} for the hemoglobin monolayer in the absence and presence of KCl, which increased with increasing [KCl]. This implied that more energy was required to compress the monolayer at higher [KCL]. The ΔG_{cm} is a characteristic energetic parameter of any monolayer at the air−liquid interface, and the cited procedure of calculation is also relevant to molecules of the systems like that forming biointerfaces.[62]

We herein add that the two-dimensional surface properties of the pluronic Langmuir monolayer film at the air/water interface in the absence and presence of di- and tripeptide as well as SDS and stearic acid have been studied in detail by Mandal et al.[63] The pluronic concentration below and above the CMC made a difference in the monolayer properties. They have also studied insoluble and soluble monolayers of geminis and the antidepressant drug hydantoin,[64] which led to concept of dry micelle formation at the interface. Monolayer of macromonomer and related polymers also demonstrated primary and secondary micelle formation at the air/water interface.

3.4. Morphology. The morphologies of pluronic L, R, and their combinations were considered important both from fundamental and application points of view. Their interactions with cells and biodistribution in the organism during application as drug carriers are reported to have morphology dependence. DLS and AFM studies on L and R were taken for their morphology evaluation.

The particle size distribution of the pluronics in solution was determined by DLS measurements in the temperature range of 20−60 °C. The temperature dependence of the hydrodynamic diameter (D_h) of 20 mM L, R, and 1:1 (L/R, mol/mol) during heating and cooling are shown in Figure 8. In the heating process, the D_h remained almost constant up to a particular temperature wherefrom it sharply increased forming a maximum in D_h both for L and L + R and then declined to some extent. The D_h of R continuously increased with temperature that corresponded to an aggregation process observed in spectrophotometry experiment (i.e., CMT) and decreased mildly afterward. Similar trends of D_h with temperature were also reported for F127 (normal pluronic) by Lindman et al.[65] The CMT values were obtained from the

dx.doi.org/10.1021/la3000729 | Langmuir 2012, 28, 7134−7146

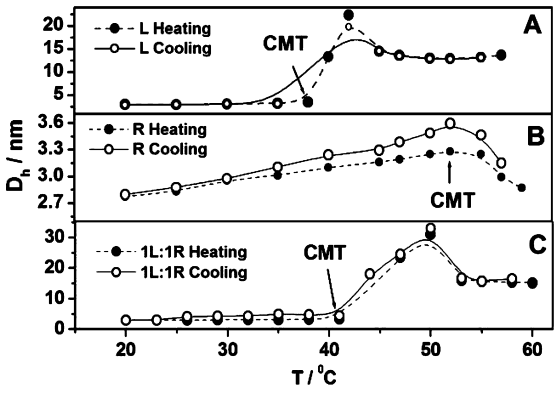

Figure 8. Temperature dependence of hydrodynamic diameter (D_h) of 20 mM pluronics. Pure L and R show weak hysteresis. Mixed L and R showed no hysteresis.

transition temperatures: for L and mixed L and R, the initial transitions corresponded to the CMT but for R the maximum D_h yielded the CMT (see Figure 8 and Table 2). Following a similar procedure, we also examined 50 mM pluronics, and the results are also given in Table 2. The DLS results agreed well with spectrophotometry. The heating and cooling values of D_h were fairly close excepting for the cooling results of R. Before CMT, the monomer molecules were non- associated and there was no change in the size. After the CMT, the monomer formed aggregates with a transition point of increasing D_h both for L and mixed pluronics (L and R). Interestingly after reaching a maximum their particle size (D_h) diminished forming smaller aggregates (it resulted from disintegration of aggregates at higher temperature). The maximum D_h for the heating process for L, R and mixed pluronics were 22.2, 3.6, and 31.5 nm, respectively. It may be noted that mixed pluronics' (1:1, mol/mol) size was larger than their individual. The average micellear size of the normal pluronics was in the range of about 15 to 35 nm, depending on the molar mass and PPO/PEO ratio.[16] A D_h value of ~4 nm for reverse pluronics was reported by Zhou et al.[37] In our DLS measurements two types of size distribution (i.e., bimodal distribution) were obtained prior to CMT of L, R and equimolar mixture of R and L. The smaller values are plotted in Figure 8, the large aggregates (100−400 nm) constituted a very small fraction. Two types of size distribution were also reported earlier for pluronics[66] and thermosensitive poly(n-butyl methacrylate)-poly(ethylene oxide) diblock copolymer.[67] Beyond CMT incorporation of the hydrophobic impurity (the diblock copolymer) into the hydrophobic core of the triblock copolymer micelles of L, R, and L + R produced a single size distribution.[68] The very high PDI values (0.55−1.0) of L below the CMT meant a non well-defined less precise system morphology.[69a] Its dramatic drop above the CMT to monodispersity (0.04−0.10) suggested well-defined assembly structure. On the other hand, R and mixed L and R produced unchanged PDI > 0.6 both below and above CMT. The structures of their aggregates were not well-defined resembling hydrophobically assembled networks of methylcellulose[69b] rather than micelle. For reverse pluronics, a variety of nonpolar conformational states became increasingly populated with loss in solvation and enhanced interaction between the hydrophobic moieties was reported.[69c]

A preliminary morphology study of the pluronics was also herein done by the AFM technique. The drying process in sample preparation was found to produce artifacts of coalesced species of large dimensions in the sample. Size analysis of such samples with statistical significance was thus uncertain. We only conclude from the study that the assembled particles of both L and R were of globular nature. We may add here that solvent removed species examined by TEM and AFM methods are reported to show appreciable morphological differences from that found by DLS experiments of their dispersed states.[70,71]

3.5. Antibacterial Activity. The antibacterial activity of L and R were tested against both *E. coli* (Gram negative) and *S. aureus* (Gram positive) bacteria. The results are given in Table 5 for 10 mM of L and R as colony forming unit (CFU). From the statistical analysis of triplicate measurements, we found that R is significantly different ($p < 0.01$) from the control samples. The results indicate microbial activity of R and inactivity of L. This is attributed to the differences of PPO and PEO block positions in the pluronics. Veyries et al.[72] also reported poloxamer 407 (pluronic F127, a normal pluronic) registered nonmicrobial activity toward both gram positive and negative bacteria. Thus, L and R (with restrictions) have prospects for uses as vehicles for carrying drugs, as biocidal materials may also have cytocompability. We may herein add that Mandal et al.[64d] have reported the minimum inhibitory concentration (MIC) of the antibacterial hydantoin drug which was very close to its CMC. In the presented study we used concentration of pluronics lower than their CMC. Determination of their MIC is thus required to check the generality of the proposition of Mandal et al.[64d]

Table 5. Antibacterial effects of 10 mM L and R

bacteria	control[a] (CFU (10^9)/mL)	L[a]	R[a]
E. coli	2.95	2.08	0.489
S. aureus	2.75	1.78	0.269

[a]Results were expressed as average ($n = 3$). $p > 0.01$.

4. COMPREHENSION AND CONCLUSION

A comprehensive account of herein determined physicochemical parameters of L and R under comparative conditions is presented in Table 6. In aqueous solution, normal pluronic L

Table 6. Comparison of Physical Parameters between L and R Pluronic

parameters	L	R
composition	$(PEO)_{10}(PPO)_{23}(PEO)_{10}$	$(PPO)_8(PEO)_{22}(PPO)_8$
M_w/g mol^{-1}	2200	1950
CMT (20 mM)	38.3 °C	52.7 °C
ΔG_{CMT}, ΔH_{CMT}, and ΔS_{CMT} for CMT[a]	−20.5, 173.8, 0.623	−21.5, 115.3, 0.420
CP (20 mM)	71 °C	61 °C
ΔG_c, ΔH_c, and ΔS_c for clouding[a]	−22.7, −405.0, −1.23	−22.0, 193.0, 0.72
D_h/nm (20 mM at 45 °C)	14.5	3.2
A_{LM}/nm^2 molecule^{-1}	8.3	19.9
ΔG_{cm} for monolayer compression[a]	211	1104

[a]ΔG and ΔH are expressed in kJ mol^{-1}, and ΔS expressed in kJ mol^{-1} K^{-1}

dx.doi.org/10.1021/la3000729 | *Langmuir* 2012, 28, 7134−7146

and reverse pluronic R form self-assemblies or micelles with characteristic CMC and CMT. At elevated temperatures than CMT they show clouding with characteristic CP values which decline with concentration for R and increase for L; the nature of their assembled structures controls these features. Solvated L, L + R, and R at low concentrations of their micelles make the systems ideal; instability and favorable aggregation of the ensembles at elevated temperature by way of desolvation at CP make them nonideal. The micellar zone between CMT and CP is larger for L than R; for equimolar mixture of L and R, the zone is intermediate as observed with reference to the studied concentration up to 50 mM (Figure 9). The temperature

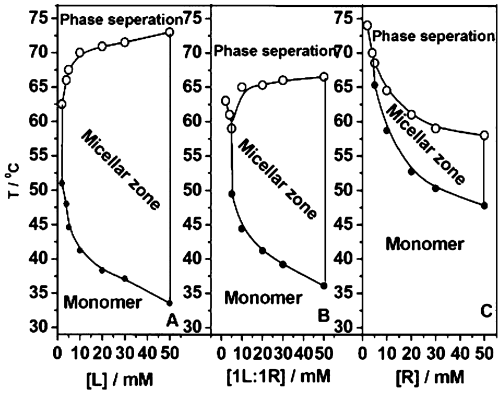

Figure 9. Temperature effect on the phase behavior of L and R, and their 1:1 mol/mol mixture. (A) L; (B) L + R at 1:1 mol ratio; (C) R. Open symbol for CP and closed symbol for CMT. Illustrations within 50 mM of pluronics are presented.

dependent monomer → micelle → phase separated state would also follow the above rationale at practicable concentration levels other than 50 mM. Different molecular ensemblings of R and their reduced solvation and loose molecular packing make differences between the concentration dependent CP of L and R. The process of micelle formation at CMT of L is less spontaneous than that of R; the corresponding enthalpy change for L is more endothermic than R with greater positive entropy change for the former. This difference accounts for greater solvation and consequent stabilization of L and its aggregates in water than that of R. The above-mentioned results for the mixtures of L and R are consequently intermediate. In the case of CP, the free energy of both L and R are nearly equal (the system with R is only moderately more spontaneous than L), but L has shown large exothermic enthalpy of clouding which for R is appreciably endothermic (the respective negative and positive entropy changes comply with the energetic directions). Clouding thus produces a compact aggregate phase for L which for R is fairly loose. At the air/water interface both L and R form monolayers with flat orientation; consequently the area described by R is greater than L. The hydrophobic $(PPO)_{23}$ of L and the $2(PPO)_8$ of R although remain at the air/water interface, by way of folding and orientation guided by steric restrictions, R describes greater area than L. The morphology of the aggregates of L and R are on the whole spherical (confirmed by AFM). DLS derived sizes are all lower than that found from AFM; the soft L and R and their assemblies grew in size by way of coalescence during AFM sample preparation by drying. Size growth by heating (found from DLS measurements) occurs in solution which moderately decreases through disaggregation beyond CMT. Interestingly, the ensembles of L have large polydispersity up to CMT; beyond CMT they become appreciably homogeneous (with low PDI). Both R and L + R remain polydisperse even beyond their CMTs. This is a prominent difference between the aggregation behavior of L and R, whereas L aggregates became nearly monodisperse at elevated temperature that of R remain practically nonvariable resembling hydrophobically assembled networks of methylcellulose rather than micelle. Pluronic L is nonbiocidal, whereas R is weakly biocidal; a detailed study (along with other pluronics) is required for evaluation of their practical uses in pharmaceutics, foods, and medicine as drug carriers. The L and R as well as their aggregates have the potential to serve as prospective templates for synthesis of nanoparticles.

AUTHOR INFORMATION

Corresponding Author

*Fax: +91-33-2414-6266. E-mail: spmcss@yahoo.com.

Notes

The authors declare no competing financial interest.

ACKNOWLEDGMENTS

B.N. thanks UGC, Government of India, for a Senior Research Fellowship. Support from Indian National Science Academy to S.P.M. is thankfully acknowledged. We thank Prof. K. P. Das, Bose Institute, for using their DLS facility. The help of Mrs. S. Mukherjee, Ms. S. Das, and Mr. S. Ghosh of Jadavpur University is thankfully acknowledged for LB, AFM, and antibacterial activity studies, respectively. The support from BASF (India) for the gift of the pluronic samples is thankfully acknowledged.

REFERENCES

(1) Chubb, C.; Draper, P. Efficacy of perfluorodecalin as an oxygen carrier for mouse and rat testes perfused in vitro. *Proc. Soc. Exp. Biol. Med.* **1987**, *184*, 489.

(2) Ho, H. O.; Chen, C. N.; Sheu, M. T. Influence of pluronic F-68 on dissolution and bioavailability characteristics of multiple-layer pellets of nifedipine for controlled release delivery. *J. Controlled Release* **2000**, *68*, 433.

(3) Lowe, K. C.; Armstrong, F. H. Oxygen-transport fluid based on perfluoro chemicals: effects on liver biochemistry. *Adv .Exp. Med. Biol.* **1990**, *277*, 267.

(4) Byars, N. E.; Allison, A. C. Adjuvant formulation for use in vaccines to elicit both cell-mediated and humoral immunity. *Vaccine* **1987**, *5*, 223.

(5) Oh, K. S.; Lee, K. E.; Han, S. S.; Cho, S. H.; Kim, D.; Yuk, S. H. Formation of core/shell nanoparticles with a lipid core and their application as a drug delivery system. *Biomacromolecules* **2005**, *6*, 1062.

(6) Samii, A. A.; Karlström, G.; Lindman, B. Influence of molecular architecture on the adsorption of poly(ethylene oxide)-poly(propylene oxide)-poly(ethylene oxide) on PDMS surfaces and implications for aqueous lubrication. *Langmuir* **1991**, *7*, 1067.

(7) Lee, S.; Iten, R.; Müller, M.; Spencer, N. D. Influence of Molecular Architecture on the Adsorption of Poly(ethylene oxide)−Poly(propylene oxide)−Poly(ethylene oxide) on PDMS Surfaces and Implications for Aqueous Lubrication. *Macromolecules* **2004**, *37*, 8349.

(8) Miyazaki, S.; Tobiyama, T.; Takada, M.; Attwood, D. Percutaneous absorption of indomethacin from pluronic F127 gels in rats. *J. Pharm. Pharmacol.* **1995**, *47*, 455.

(9) Khalil, E. A.; Afifi, F. U.; Al-Hussaini, M. Evaluation of the wound healing effect of some Jordanian traditional medicinal plants formulated in Pluronic F127 using mice (Mus musculus). *J. Ethnopharmacol* **2007**, *109*, 104.

(10) Gaymalov, Z. Z.; Yang, Z.; Pisarev, V. M.; Alakhov, V. Y.; Kabanov, A. V. The effect of the nonionic block copolymer pluronic P85 on gene expression in mouse muscle and antigen-presenting cells. *Biomaterials* **2009**, *30*, 1232.
(11) Jung, H.; Park, K.; Han, D. K. Preparation of TGF-β1-conjugated biodegradable pluronic F127 hydrogel and its application with adipose-derived stem cells. *J. Controlled Release* **2010**, *147*, 84.
(12) Kretlow, J. D.; Klouda, L.; Mikos, A. G. Injectable matrices and scaffolds for drug delivery in tissue engineering. *Adv. Drug Delivery Rev.* **2007**, *59*, 263.
(13) Muszanska, A. K.; Busscher, H. J.; Herrmann, A.; van der Mei, H. C.; Norde, W. Pluronic−lysozyme conjugates as anti-adhesive and antibacterial bifunctional polymers for surface coating. *Biomaterials* **2011**, *32*, 6333.
(14) Palazzo, G.; Fiorentino, D.; Colafemmina, G.; Ceglie, A.; Carretti, E.; Dei, L.; Baglioni, P. Nanostructured fluids based on propylene carbonate/water mixtures. *Langmuir* **2005**, *21*, 6717.
(15) Wu, J.; Xu, Y.; Dabros, T.; Hamza, H. Effect of EO and PO positions in nonionic surfactants on surfactant properties and demulsification erformance. *Colloids Surf. A* **2005**, *252*, 79.
(16) Kabonova, A. K.; Nazarova, I. R.; Astafieva, I. V.; Batrakova, E. V.; Alakhov, V. Y.; Yaroslavo, A. A.; Kabanov, A. V. Micelle formation and solubilization of fluorescent probes in poly (oxyethylene-b-oxypropylene-b-oxyethylene) solutions. *Macromolecules* **1995**, *28*, 2303.
(17) Alexandridis, P.; Holzwarth, J. F.; Hatton, T. A. Micellization of poly (ethylene oxide)-poly (propylene oxide)-poly (ethylene oxide) triblock copolymers in aqueous solutions: thermodynamics of copolymer association. *Macromolecules* **1994**, *27*, 2414.
(18) Alexandridis, P.; Athanassiou, V.; Fukuda, S.; Hatton, T. A. Surface activity of poly (ethylene oxide)-block-poly (propylene oxide)-block-poly (ethylene oxide) copolymers. *Langmuir* **1994**, *10*, 2604.
(19) Liu, T. Y.; Hu, S. H.; Liu, K. H.; Shaiu, R. S.; Liu, D. M.; Chen, S. Y. Instantaneous drug delivery of magnetic/thermally sensitive nanospheres by a high-frequency magnetic field. *Langmuir* **2008**, *24*, 13306.
(20) Florent, M.; Cohen, R. S.; Goldfarb, D.; Rozen, R. Y. Block Copolymer-Mediated Synthesis of Size-Tunable Gold Nanospheres and Nanoplates. *Langmuir* **2008**, *24*, 13186.
(21) (a) Prasad, M.; Moulik, S. P.; Chisholm, D.; Palepu, R. Influence of Hydrotropes and Glycols on the Clouding Behavior of Surfactants (TritonX 100 and Brij 56) and Polymers (Polyvinylmethyl Ether and Triblock Co-Polymer, Pluronic 85). *J. Oleo. Sci.* **2003**, *52*, 523. (b) Sardar, N.; Ali, M. S.; Kamil, M. Kabir-ud-Din. Phase Behavior of Nonionic Polymer Hydroxypropylmethyl Cellulose: Effect of Gemini and Single-Chain Surfactants on the Energetics at the Cloud Point. *J. Chem. Eng. Data* **2010**, *55*, 4990. (c) Majhi, P. R.; Mukherjee, K.; Moulik, S. P.; Sen, S.; Sahu, N. P. Solution Properties of a Saponin (Acaciaside) in the Presence of Triton X-100 and Igepal. *Langmuir* **1999**, *15*, 6624.
(22) Dan., A.; Ghosh, S.; Moulik, S. P. The Solution Behavior of Poly(vinylpyrrolidone): Its Clouding in Salt Solution, Solvation by Water and Isopropanol, and Interaction with Sodium Dodecyl Sulfate. *J. Phys. Chem. B* **2008**, *112*, 3617.
(23) Akita, S.; Takeuchi, H. Cloud-point extraction of organic compounds from aqueous solutions with non-ionic surfactant. *Sep. Sci. Technol.* **1995**, *30*, 833.
(24) Cordero, B. M.; Pavon, J. L. P.; Pinto, C. G.; Laespada, M. E. F. Cloud point methodology: A new approach for preconcentration and separation in hydrodynamic systems of analysis. *Talanta* **1993**, *40*, 1703.
(25) Alexandridis, P.; Holzwarth, J. F. Differential scanning calorimetry investigation of the effect of salts on aqueous solution properties of an amphiphilic block copolymer (Poloxamer). *Langmuir* **1997**, *13*, 6074.
(26) Mata, J. P.; Majhi, P. R.; Guo, C.; Liu, H. Z.; Bahadur, P. Concentration, temperature, and salt-induced micellization of a triblock copolymer Pluronic L64 in aqueous media. *J. Colloid Interface Sci.* **2005**, *292*, 548.
(27) Jain, N. J.; George, A.; Bahadur, P. Effect of salt on the micellization of pluronic P65 in aqueous solution. *Colloids Surf. A* **1999**, *157*, 275.
(28) Bharatiya, B.; Guo, C.; Ma, J. H.; Kubota, O.; Nakashima, K.; Bahadur, P. Urea-induced demicellization of Pluronic L64 in water. *Colloid Polym. Sci.* **2009**, *287*, 63.
(29) Maskarinec, S. A.; Lee, K. Y. C. Comparative study of poloxamer insertion into lipid monolayers. *Langmuir* **2003**, *19*, 1809.
(30) Yasuda, S.; Townsend, D. E.; Michele, E. G.; Favre, E. G.; Day, S. M.; Metzger, J. M. Dystrophic heart failure blocked by membrane sealant poloxamer. *Nature* **2005**, *436*, 1025.
(31) Chang, L. C.; Chang, Y. Y.; Gau, C. S. On the temperature dependence of intrinsic surface protonation equilibrium constants: an extension of the revised MUSIC model. *J. Colloid Interface Sci.* **2008**, *322*, 263.
(32) (a) Sakai, T.; Kaneko, Y.; Tsujii, K. Premicellar aggregation of fatty acid N-methylethanolamides in aqueous solutions. *Langmuir* **2006**, *22*, 2039. (b) Lin, Y.; Alexandridis, P. Cosolvent Effects on the Micellization of an Amphiphilic Siloxane Graft Copolymer in Aqueous Solutions. *Langmuir* **2002**, *18*, 4220. (c) Li, X.; Wettig, S. D.; Wang, C.; Foldvarib, M.; Verrall, R. E. Long-range corrected hybrid density functionals with damped atom−atom dispersion corrections. *Phys. Chem. Chem. Phys.* **2005**, *7*, 3172.
(33) (a) James, J.; Vellaichami, S.; Krishnan, R. S. G.; Samikannu, S.; Mandal, A. B. Interaction of poly (ethylene oxide)−poly (propylene oxide)−poly(ethylene oxide) triblock copolymer of molecular weight 2800 with sodium dodecylsulfate (SDS) micelles: some physicochemical studies. *Chem. Phys.* **2005**, *312*, 275. (b) James, J.; Ramalechume, C.; Mandal, A. B. Self-diffusion studies on PEO-PPO-PEO triblock copolymer micelles in SDS micelles and vice versa using cyclic voltametry. *Chem. Phys. Lett.* **2005**, *405*, 84.
(34) (a) Phani Kumar, B. V. N.; Priyadharsini, S. U.; Prameela, G. K. S.; Mandal, A. B. NMR investigations of self-aggregation characteristics of SDS in a model assembled tri-block copolymer solution. *J. Colloid Interface Sci.* **2011**, *360*, 154. (b) James, J.; Mandal, A. B. The aggregation of Tyr-Phe dipeptide and Val-Tyr-Val tripeptide in aqueous solution and in the presence of SDS and PEO−PPO−PEO triblock copolymer: Fluorescence spectroscopic studies. *J. Colloid Interface Sci.* **2011**, *360*, 600. (c) James, J.; Mandal, A. B. Micelle formation of Tyr-Phe dipeptide and Val-Tyr-Val tripeptide in aqueous solution and their influence on the aggregation of SDS and PEO−PPO−PEO copolymer micelles. *Colloids Surf. B* **2011**, *84*, 172.
(35) Trong, L. C. P.; Djabourov, M.; Ponton, A. Mechanisms of micellization and rheology of PEO−PPO−PEO triblock copolymers with various architectures. *J. Colloid Interface Sci.* **2008**, *328*, 278.
(36) Pojják, K.; Mészáros, R. Preparation of Stable Electroneutral Nanoparticles of Sodium Dodecyl Sulfate and Branched Poly-(ethylenimine) in the Presence of Pluronic F108 Copolymer. *Langmuir* **2011**, *27*, 14797.
(37) Zhou, Z.; Chu, B. Phase Behavior and Association Properties of Poly(oxypropylene)-Poly(oxyethylene)-Poly(oxypropylene) Triblock Copolymer in Aqueous Solution. *Macromolecules* **1994**, *27*, 2025.
(38) Huff, A.; Patton, K.; Odhner, H.; Jacobs, D. T.; Clover, B. C.; Greer, S. C. Micellization and Phase Separation for Triblock Copolymer 17R4 in H_2O and in D_2O. *Langmuir* **2011**, *27*, 1707.
(39) D'Errico, G.; Paduano, L.; Khan, A. Temperature and concentration effects on supramolecular aggregation and phase behavior for poly(propylene oxide)-*b*-poly(ethylene oxide)- *b*-poly-(propylene oxide) copolymers of different composition in aqueous mixtures, 1. *J. Colloid Interface Sci.* **2004**, *279*, 379.
(40) Li, L.; Lim, L. H.; Wang, Q.; Jiang, S. P. Thermoreversible micellization and gelation of a blend of pluronic polymers. *Polymer* **2008**, *49*, 1952.
(41) Naskar, B.; Ghosh, S.; Nagadome, S.; Sugihara, G.; Moulik, S. P. Behavior of the Amphiphile CHAPS Alone and in Combination with the Biopolymer Inulin in Water and Isopropanol-Water Media. *Langmuir* **2011**, *27*, 9148.
(42) Maiti, K.; Bhattacharya, S. C.; Moulik, S. P.; Panda, A. K. Physicochemistry of the binary interacting mixtures of cetylpyridinium

chloride (CPC) and sodium dodecylsulfate (SDS) with special reference to the catanionic ion-pair (coacervate) behavior. *Colloids Surf. A* **2010**, *355*, 88.
(43) Lemay, M. J.; Choquette, J.; Delaquis, P. J.; Gariépy, C.; Rodrigue, N.; Saucier, L. Antimicrobial effect of natural preservatives in a cooked and acidified chicken meat model. *Int. J. Food Microbiol.* **2002**, *78*, 217.
(44) Liang, X.; Guo, C.; Ma, J.; Wang, J.; Chen, S.; Liu, H. Temperature-dependent aggregation and disaggregation of poly (ethylene oxide)-poly (propylene oxide)-poly (ethylene oxide) block copolymer in aqueous solution. *J. Phys. Chem. B* **2007**, *111*, 13217.
(45) Bouchemal, K.; Agnely, F.; Koffi, A.; Ponchel, G. A concise analysis of the effect of temperature and propanediol-1, 2 on Pluronic F127 micellization using isothermal titration microcalorimetry. *J. Colloid Interface Sci.* **2009**, *338*, 169.
(46) Li, Y.; Xu, R.; Couderc, S.; Bloor, D. M.; Wyn-Jones, E.; Holzwarth, J. F. Binding of Sodium Dodecyl Sulfate (SDS) to the ABA Block Copolymer Pluronic F127 ($EO_{97}PO_{69}EO_{97}$):F127 Aggregation Induced by SDS. *Langmuir* **2001**, *17*, 183.
(47) (a) Taboada, P.; Mosquera, V.; Attwood, D.; Yangc, Z.; Boothc, C. Enthalpy of micellisation of a diblock copoly (oxyethylene/oxypropylene) by isothermal titration calorimetry. Comparison with the van't Hoff value. *Phys. Chem. Chem. Phys.* **2003**, *5*, 2625. (b) Raju, B. B.; Winnik, F. M.; Morishima, Y. A Look at the Thermodynamics of the Association of Amphiphilic Polyelectrolytes in Aqueous Solutions: Strengths and Limitations of Isothermal Titration Calorimetry. *Langmuir* **2001**, *17*, 4416.
(48) (a) Yang, L.; Alexandridis, P.; Steytler, D. C.; Kositza, M. J.; Holzwarth, J. F. Small-Angle Neutron Scattering Investigation of the Temperature-Dependent Aggregation Behavior of the Block Copolymer Pluronic L64 in Aqueous Solution. *Langmuir* **2000**, *16*, 8555. (b) Ruthstein, S.; Raitsimring, A. M.; Bitton, R.; Frydman, V.; Godte, A.; Goldfarb, D. Distribution of guest molecules in Pluronic micelles studied by double electron electron spin resonance and small angle X-ray scattering. *Phys. Chem. Chem. Phys.* **2009**, *11*, 148.
(49) Batrakova, E. V.; Lee, S.; Li, S.; Venne, A.; Alakhov, V. Yu.; Kabanov, A. V. Fundamental relationships between the composition of pluronic block copolymers and their hypersensitization effect in MDR cancer cells. *Pharm. Res.* **1999**, *16*, 1375.
(50) Prasad, M.; Chakraborty, I.; Rakshit, A. K.; Moulik, S. P. Critical Evaluation of Micellization Behavior of Nonionic Surfactant MEGA 10 in Comparison with Ionic Surfactant Tetradecyltriphenylphosphonium Bromide Studied by Microcalorimetric Method in Aqueous Medium. *J. Phys. Chem. B* **2006**, *110*, 9815.
(51) Moulik, S. P.; Mitra, D. Amphiphile self-aggregation: An attempt to reconcile the agreement−disagreement between the enthalpies of micellization determined by the van't Hoff and Calorimetry methods. *J. Colloid Interface Sci.* **2009**, *337*, 569 and references therein..
(52) Tsui, H. W.; Wang, J. H.; Hsu, Y. H.; Chen, L. J. Study of heat of micellization and phase separation for Pluronic aqueous solutions by using a high sensitivity differential scanning calorimetry. *Colloid Polym. Sci.* **2010**, *288*, 1687.
(53) (a) Dai, S.; Tam, K. C.; Li, L. Isothermal Titration Calorimetric Studies on Interactions of Ionic Surfactant and Poly(oxypropylene)−Poly(oxyethylene)−Poly(oxypropylene) Triblock Copolymers in Aqueous Solutions. *Macromolecules* **2001**, *34*, 7049. (b) Iqbal, M.; Chung, Y.; Tae, G. An Enhanced Synthesis of Gold Nanorods by the Addition of Pluronic (F-127) via a Seed Mediated Growth Process. *J. Mater. Chem.* **2007**, *17*, 335. (c) Dey, S.; Adhikari, A.; Mandal, U.; Ghosh, S.; Bhattacharya, K. A Femtosecond Study of Excitation Wavelength Dependence of a Triblock Copolymer−Surfactant Supramolecular Assembly: $(PEO)_{20}$−$(PPO)_{70}$−$(PEO)_{20}$ and CTAC. *J. Phys. Chem. B* **2008**, *112*, 5020. (d) Couderc, S.; Li, Y.; Bloor, D. M.; Holzwarth, J. F.; Wyn-Jones, E. Interaction between the Nonionic Surfactant Hexaethylene Glycol Mono-*n*-dodecyl Ether ($C_{12}EO_6$) and the Surface Active Nonionic ABA Block Copolymer Pluronic F127 ($EO_{97}PO_{69}EO_{97}$)—Formation of Mixed Micelles Studied Using Isothermal Titration Calorimetry and Differential Scanning Calorimetry. *Langmuir* **2001**, *17*, 4818. (e) Mahajan, R. K.; Kaur, N.; Bakshi, M. S. Cyclic Voltammetry Investigation of the Mixed Micelles of Cationic Surfactants with Pluronic F68 and Triton X-100. *Colloids Surf. A* **2005**, *255*, 33.
(54) Basu Ray, G.; Chakraborty, I.; Ghosh, S.; Moulik, S. P. Self-aggregation of alkyltrimethylammonium bromides (C_{10}-, C_{12}-, C_{14}-, and C_{16}TAB) and their binary mixtures in aqueous medium: a critical and comprehensive assessment of interfacial behavior and bulk properties with reference to two types of micelle formation. *Langmuir* **2005**, *21*, 10958.
(55) Wang, Z. Interactions between an anionic fluorosurfacant and a PEO-PPO-PEO copolymer in aqueous solutions. *J. Surfact. Deterg.* **2010**, *13*, 97.
(56) Zhang, Y.; Lam, Y. M. Using nanoparticles to enable simultaneous radiation and photodynamic therapies for cancer treatment. *J. Nano. Sci. Nano. Technol.* **2006**, *6*, 1.
(57) Almgren, M.; Brown, W.; Hvidt, S. Self-aggregation and phase behavior of poly (ethylene oxide)-poly (propylene oxide)-poly (ethylene oxide) block copolymers in aqueous solution. *Colloid Polym. Sci.* **1995**, *273*, 2.
(58) Chowdhrya, B. Z.; Snowdena, J. M.; Leharne, S. A. A scanning calorimetric investigation of phase transitions in a PPO-PEO-PPO block copolymer. *Eur. Polym. J.* **1999**, *35*, 273.
(59) Paterson, I.; Armstrong, J.; Chowdhry, B.; Leharne, S. Thermodynamic Model Fitting of the Calorimetric Output Obtained for Aqueous Solutions of Oxyethylene− Oxypropylene−Oxyethylene Triblock Copolymers. *Langmuir* **1997**, *13*, 2219.
(60) Chang, L.; Chang, Y.; Gau, C. Interfacial properties of pluronics and the interaction between pluronic and cholesterol/DPPC mixed monolayers. *J. Colloid Interface Sci.* **2008**, *322*, 263.
(61) Mahato, M.; Pal, P.; Kamilya, T.; Sarkar, R.; Chaudhuri, A.; Talapatra, G. B. Influence of KCl on the interfacial activity and conformation of hemoglobin studied by Langmuir−Blodgett technique. *Phys. Chem. Chem. Phys.* **2010**, *12*, 12997.
(62) Lu, J. R.; Su, T, J.; Georganopoulou, D.; Williams, D. E. Interfacial Dissociation and Unfolding of Glucose Oxidase. *J. Phys. Chem. B* **2003**, *107*, 3954.
(63) James, J.; Ramalechume, C.; Mandal, A. B. Two-dimensional surface properties of PEO−PPO−PEO triblock copolymer film at the air/water interface in the absence and presence of Tyr-Phe dipeptide, Val-Tyr-Val tripeptide, SDS and stearic acid. *Colloids Surf. B* **2011**, *82*, 345.
(64) (a) Geetha, B.; Mandal, A. B. 2-Dimensional surface properties of ω-methoxy poly(ethylene glycol) macromonomer and homopolymer at the air−water interface. *Chem. Phys. Lett.* **2000**, *318*, 35. (b) Krishnan, R. S. G.; Thennarasu, S.; Mandal, A. B. Self-Assembling Characteristics of A New Nonionic Gemini Surfactant. *J. Phys. Chem. B* **2004**, *108*, 8806. (c) Geetha, B.; Mandal, A. B. Two-Dimensional Surface Properties of the Mixed Film of *o*-Methoxy Poly(ethylene glycol) Macromonomer with Stearic Acid at the Air-Water Interface in Absence and Presence of SDS at Different Temperatures. *Langmuir* **2000**, *16*, 3957. (d) Mandal, A.; Krishnan, R. S. G.; Thennarasu, S.; Panigrahib, S.; Mandal, A. B. Two-dimensional surface properties of an antimicrobial hydantoin at the air−water interface: An experimental and theoretical study. *Colloids Surf. B* **2010**, *79*, 136.
(65) Malmsten, M.; Lindman, B. Self-assembly in aqueous block copolymer solution. *Macromolecules* **1992**, *25*, 5440.
(66) Patel, K.; Bahadur, P.; Guo, C.; Ma, J. H.; Liu, H. Z.; Nakashima, K. Salt induced micellization of pluronics F88 in water. *J. Disp. Sci. Technol.* **2008**, *29*, 748.
(67) Lee, H. N.; Lodge, T. P. Poly(*n*-butyl methacrylate) in Ionic Liquids with Tunable Lower Critical Solution Temperatures (LCST). *J. Phys. Chem. B* **2011**, *115*, 1971.
(68) Penders, M. H. G. M.; Nilsson, S.; Piculell; Lindman, B. Clouding and diffusion of a poly(ethylene oxide)-poly(propylene oxide)- poly(ethylene oxide) block copolymer in agarose gels and solutions. *J. Phys. Chem.* **1994**, *98*, 5508.
(69) (a) Hassan, P. A.; Kulshreshtha, S. K. Modification to the cumulant analysis of polydispersity. *J. Colloid Interface Sci.* **2006**, *300*, 744. (b) Li, L.; Thangamathesvaran, M.; Yue, C. Y.; Tam, K. C.; Hu,

X.; Lam, Y. C. Gel network structure of methylcellulose in water. *Langmuir* **2001**, *17*, 8062. (c) Hergeth, W. D.; Alig, I.; Lange, J.; Lochmann, J. R.; cherzer, T. On the molecular mechanism of clouding in aqueous solution of poly(oxyethylene)-poly(oxypropylene)-poly-(oxyethylene) triblock copolymers. *Makromol. Chem. Macromol. Symp.* **1991**, *52*, 289.

(70) Kohori, F.; Sakai, K.; Aoyagi, T.; Yokoyama, M.; Sakurai, Y.; Okano, T. Preparation and characterization of thermally responsive block copolymer micelles comprising poly(*N*-isopropylacrylamide-*b*-dl-lactide). *J. Controlled Release* **1998**, *55*, 87.

(71) Naskar, B.; Dan, A.; Ghosh, S.; Moulik, S. P. Characteristic physicochemical features of the biopolymer inulin in solvent added and depleted states. *Carbohydr. Polym.* **2010**, *81*, 700.

(72) Veyries, M. L.; Faurisson, F.; Guillou, M. L. J.; Rouveix, B. In vitro activities of daptomycin, vancomycin, linezolid, and quinupristin-dalfopristin against staphylococci and enterococci, including vancomycin-intermediate and-resistant strains. *Antimicrob. Agents Chemother.* **2000**, *44*, 1093.